HHS Public Access

Author manuscript

Biomaterials. Author manuscript; available in PMC 2020 June 01.

Published in final edited form as:

Biomaterials. 2019 June ; 204: 59–69. doi:10.1016/j.biomaterials.2019.03.003.

MiR-145 mediates cell morphology-regulated mesenchymal stem cell differentiation to smooth muscle cells

Yi-Ting Yeh[a,b,c,1], **Josh Wei**[a,b,1], **Satenick Thorossian**[b], **Katherine Nguyen**[a,b], **Clarissa Hoffman**[a,b], **Juan C. del Álamo**[b,c], **Ricardo Serrano**[c], **Yi-Shuan Julie Li**[a,b], **Kuei-Chun Wang**[a,b,**], **Shu Chien**[a,b,*]

[a]Department of Bioengineering, University of California, San Diego, La Jolla, CA, 92093, United States

[b]Institute of Engineering in Medicine, University of California, San Diego, La Jolla, CA, 92093, United States

[c]Department of Mechanical and Aerospace Engineering, University of California, San Diego, La Jolla, CA, 92093, United States

Abstract

The use of biochemical signaling to derive smooth muscle cells (SMCs) from mesenchymal stem cells (MSCs) has been explored, but the induction of a fully functional SMC phenotype remains to be a major challenge. Cell morphology has been shown to regulate MSC differentiation into various lineages, including SMCs. We engineered substrates with microgrooves to induce cell elongation to study the mechanism underlying the MSC shape modulation in SMC differentiation. In comparison to those on flat substrates, MSCs cultured on engineered substrates were elongated with increased aspect ratios for both cell body and nucleus, as well as augmented cytoskeletal tensions. Biochemical studies indicated that the microgroove-elongated cells expressed significantly higher levels of SMC markers. MicroRNA analyses showed that up-regulation of miR-145 and the consequent repression of KLF4 in these elongated cells promoted MSC-to-SMC differentiation. Rho/ROCK inhibitions, which impair cytoskeletal tension, attenuated cell and nuclear elongations and disrupted the miR-145/KLF4 regulation for SMC differentiation. Furthermore, cell traction force measurements showed that miR-145 is essential for the functional contractility in the microgroove-induced SMC differentiation.

*Corresponding author. Department of Bioengineering and Insitute of Engineering in Medicine, University of California, San Diego, La Jolla, CA, 92093, United States. shuchien@eng.ucsd.edu (S. Chien). **Corresponding author. Department of Bioengineering and Institute of Engineering in Medicine, University of California, San Diego, La Jolla, CA, 92093, United States. k9wang@ucsd.edu (K.-C. Wang).

[1]First authors.

Author contributions

Y.-T.Y., K.-C.W., and S.C. conceived the project and designed the analysis; Y.-T.Y., J.W., S.T., K.N., C.H., and K.-C.W. performed the experiments and collected the data; J.d Á. and R.S. contributed to analysis tool; Y.-T.Y., Y.-S.L., and K.-C.W. performed the analysis; Y.-T.Y., Y.S.L., K.-C.W., and S.C. wrote the paper.

Data availability statement

The raw/processed data that support the findings of this study are available from the corresponding authors, K.-C.W. and S.C., upon reasonable request.

Appendix A. Supplementary data

Supplementary data to this article can be found online at https://doi.org/10.1016/j.biomaterials.2019.03.003.

Collectively, our findings demonstrate that, through a Rho-ROCK/miR-145/KLF4 pathway, the elongated cell shape serves as a decisive geometric cue to direct MSC differentiation into functional SMCs.

Keywords

Mesenchymal stem cell; Smooth muscle cell; Cell shape modulation; miR-145

1. Introduction

Vascular smooth muscle cells (SMCs) residing in the tunica media layer of blood vessel wall play a key role in regulating vascular tone. In response to arterial injuries such as angioplasty, stenting, or vessel grafting, SMCs undergo phenotypic switch from a physiological contractile phase to a pathological proliferative phase, leading to intima hyperplasia and ultimately artery restenosis and graft failure [1]. Recent studies have shown that, in addition to the synthetic SMCs migrating from media layer, bone marrow-derived mesenchymal stem cells (MSCs) are recruited to the sites of arterial injury and contribute to the post-injury repair process [2–4]. These MSCs are capable of differentiating into smooth muscle-like cells *in vitro* and *in vivo* and hence hold a great potential for tissue-engineered vascular grafts and regenerative therapy.

The fate of MSCs can be regulated by the biomechanical properties of the local tissue microenvironments. For example, MSCs cultured on elastomeric matrices mimicking tissue stiffness can direct MSC differentiation toward specific lineages as soft substrates with the rigidity of 0.1–1 kPa promote neuronal differentiation, whereas hard substrates at 25–40 kPa induce osteoblast differentiation [5]. In addition to substrate rigidity, cell morphology, the degree of cell spreading, and the resulting cytoskeletal tension change are functions of the topography in the extracellular matrix and have been demonstrated as critical modulators to guide MSC differentiation [6,7]. McBeath et al. reported that MSCs cultured on small micro-patterned islands differentiate into adipocytes, while the ones on large islands primarily turn into osteoblasts [6]. Killian et al. demonstrated that patterning MSCs to different geometric shapes (flower vs. star shapes) but with the same area led to distinct differentiations toward adipocytes or osteoblasts, respectively [7]. Induction of MSC or SMC elongation, which mimics the contractile SMC phenotype, has been shown to promote SMC differentiation, although the underlying mechanism is not clearly understood [8–10].

MicroRNAs (miRNAs) are post-transcriptional regulators of gene expression and play pivotal roles in modulating a wide variety of biological processes, including stem cell renewal and differentiation [11]. In muscle cells, a group of miRNAs known as myomiRs (including miR1, −133, −206 and −208) are involved in muscle homeostasis and development [12]. In SMCs, altered expressions of miR-1, −21, −23, −125b, −143, −145 and −155 have been shown to mediate the phenotypic plasticity of SMCs [13,14]. Among these miRNAs, miR-143/145 cluster promotes the contractile phenotype of SMCs by up-regulating SMC contractile markers via targeting Krüppel-like factor 4/5 (KLF4/5) [14,15]. Hence, up-regulation of miR-143/145 in MSCs *in vitro* may direct their differentiation

into SMCs [16]. Furthermore, recent studies have identified a panel of mechano-sensitive miRNAs relaying the signal transduction to modulate vascular homeostasis in response to the mechanical stimuli such as fluid shear stress and cyclic stretch [17–19]. In this study, we hypothesized that the shape modulation of MSCs to an elongated morphology can induce a differential expression profile of miRNAs to regulate gene expression post-transcriptionally for their differentiation into SMCs.

In the present study, we used the soft lithography technique to fabricate polydimethylsiloxane (PDMS) microgrooved substrates to constrain MSCs to an elongated cell shape and examined the MSC-to-SMC differentiation process. We found that the resulting increases in cell and nuclear aspect ratios had a synergistic effect with TGF-β1 treatment on the MSC differentiation into SMCs. Through the screening of myomiRs and miRNAs involved in smooth muscle plasticity, we identified miR-145 as a critical mechano-transducer that mediates the elongated cell shape-induced MSC-to-SMC differentiation. By pharmacological inhibition of the Rho/ROCK pathway, we demonstrated that the miR-145-mediated SMC differentiation was regulated by cell shape-induced Rho/ROCK signaling. Using Traction Force Microscopy (TFM), we found that the cell elongation-induced miR-145 was necessary for the contractile function of differentiated SMCs. Our findings serve to advance the understanding of mechano-biochemical mechanisms for MSC-to-SMC differentiation, thus contributing to MSC-based regenerative vascular medicine.

2. Materials and Methods

2.1. Mesenchymal stem cell culture

Human bone marrow-derived MSCs (Cell Applications) were maintained in human marrow stromal cell growth medium (MSCGM, Cell Applications) and passaged once cells reached 80–90% confluence. MSCs within passages 5–8 were used in all experiments.

2.2. PDMS microgrooved substrate fabrication

A silicon wafer (University Wafer) was prebaked for 5 min at 95 °C before plasma etching the surface (Technics PEIIB planar etcher). Photoresist (SU-8 2005, MicroChem) was spin-coated onto the wafer to desired thickness and soft baked at 95 °C for 2 min. The wafer was exposed to ultraviolet (UV) light with a photomask patterned with 10, 25, and 50 μm of chrome channels using the Karl Suss MA6 Mask Aligner. After hard baking at 95 °C for 3 min, UV light induced the cross-linking of the exposed photoresist. The wafer was then washed in SU-8 developer for 1 min followed by isopropyl alcohol for 1 min, and then rinsed with water and air-dried to obtain the wafer mold. PDMS (Sylgard 184, Dow Corning) base and curing agents were mixed at 10:1 ratio and poured over the patterned wafer mold to form the features. The PDMS was cured for 1 h at 60 °C before it was peeled off. After demolding, the patterned PDMS substrates were surface-activated by UV ozone (JetLight) to improve surface hydrophilicity.

2.3. Cell culture conditions on PDMS substrates

The microgrooved or flat PDMS substrates were coated with 50 μg/ mL fibronectin (FN, Sigma) overnight. MSCs were seeded onto the substrates at a density of 1×10^4 cells/cm^2.

For cell morphology imaging, MSCs were cultured on the microgrooved or flat substrates for 24 h in DMEM media (DMEM, 10% FBS, 100 U/mL penicillin, and 100 μg/mL streptomycin) supplemented with 5 ng/mL TGF-β1 (Peprotech). For inhibiting Rho/ROCK signaling, cells were treated with C3 exoenzyme (a Rho inhibitor, 1 μg/mL) or Y-27632 (a ROCK inhibitor, 20 μM, Abcam) for 24 h. For all other experiments, MSCs were cultured on substrates for 3 days.

2.4. Immunofluorescence and confocal microscopy

Cells were fixed in 4% paraformaldehyde and permeabilized with 0.25% Triton X-100 for 10 min, followed by blocking with 5% BSA and incubating with primary/secondary antibodies. 4′,6-diamidino-2-phenylindole (DAPI, Sigma) was used for nucleus staining, and FITC-phalloidin (Invitrogen) was used for F-actin staining and cell morphology analysis. Three-dimensional (3-D) images were acquired in the form of Z-stacks by a confocal scanning microscope (Olympus IX81) with a cooled CCD (Hamamatsu), controlled by the Metamorph software (Molecular Devices) and a 40× NA 1.35 oil immersion objective. These 3-D images were rendered by using the Volocity software (PerkinElmer). The 2-D images were taken under an epi-fluorescence microscope (Olympus IX70) for quantifying cell morphology parameters.

2.5. Western blots

Cell lysate was prepared in modified RIPA buffer (50 mM Tris pH 7.4, 1% NP-40, 0.1% sodium deoxycholate, 0.1% SDS, and 150 mM NaCl) supplemented with protease inhibitors, quantified by Bradford protein assay (Bio-Rad), separated by SDS-PAGE, followed by transferring onto nitrocellulose membranes and blocked with 5% BSA. The membranes were then incubated with primary antibodies including MYH11 (ab53219, Abcam), α-smooth muscle actin (α-SMA) (1A4, Sigma), SM-22 (ab14106, Abcam), KLF4 (PA5–23184, Invitrogen) and GAPDH (14C10, Cell Signaling), followed by incubations with the respective horseradish peroxidase-conjugated secondary antibodies. Blots were developed using enhanced chemiluminescence substrate (ThermoFisher) and imaged in a gel documentation system (Alpha Innotech), followed by quantification using ImageJ.

2.6. Quantitative RT-PCR

Total RNA was isolated using the TRIzol reagent (ThermoFisher). Reverse transcription (RT) was performed by using oligo(dT) primer. Quantitative RT-PCR (qRT-PCR) was performed with custom primers (Integrated DNA Technologies) (SI Table1) in a CFX Connect™ real-time PCR detection system (BioRad). The expression levels of miRNAs were determined using TaqMan® MicroRNA Assays (ThermoFisher) according to the manufacturer's protocol. GAPDH and RNU48 were used as the internal controls.

2.7. MiRNA transfection

Pre-miR™ miRNA precursors and Anti-miR™ miRNA inhibitors (Ambion) were used in the gain-of-function and loss-of-function experiments along with the respective negative control molecules. The oligonucleotides were reverse transfected in a 6-well plate using RNAiMAX (ThermoFisher) in Opti-MEM (ThermoFisher).

2.8. Polyacrylamide gel preparation and image acquisition

To perform TFM, an elastic polyacrylamide gel with embedded fluorescent beads was fabricated in glass-bottom dishes. The dishes were treated with 0.1 M NaOH, followed by 3% 3-aminopropyltrimethoxysilane (APES, Sigma) in 95% ethanol, and then baked. The polyacrylamide solution (5% acrylamide, 0.3% bis-acrylamide) containing 0.2 μm fluorescent beads (3%, ThermoFisher) was polymerized with the addition of APS and TEMED on a coverglass for curing at room temperature for 40 min. The coverglass was then removed, and the Sulfo-SANPAH crosslinker and FN (50 μg/mL) were added to the gel surface and activated by UV cross-linking. The polyacrylamide gel thickness was measured by confocal microscopy. The Young's modulus of bis-acrylamide polyacrylamide gel is ~8 kPa, and the Poisson ratio is ~0.48. The cells were cultured on the microgrooved or flat substrates for 3 days prior to trypsinization and sub-cultured onto the polyacrylamide gels for 24 h for TFM measurements.

2.9. Traction force microscopy (TFM)

The forces exerted by the cells on the substrate were measured using the TFM method as previously described [20,21]. Around each cell, a thin layer near the top surface of the substrate containing fluorescent beads was imaged in the form of a Z-stack using a confocal microscope. Each stack consisted of 38 planes separated by 0.4 μm in the z direction. The substrate deformations were calculated using the particle image velocity to track the motion of the beads between each Z-stack in which the substrate was deformed and a non-deformed, load-free reference Z-stack. The non-deformed Z-stack was obtained after the cells were removed at the end of experiment. For each experiment, the instantaneous and reference, *Z*-stacks were divided into 3-D interrogation boxes of 32 × 32 × 12 pixels in the *x*, *y*, and *z* directions respectively, to balance resolution and the signal-to-noise ratio. These settings provided a Nyquist spatial resolution of 2 μm in all three directions. Using these measurements, we solved the elastostatic equation for the substrate, which provide the 3-D traction stress vector on the top surface of the substrate and the traction forces exerted by the cells.

2.10. Statistical analysis

For comparisons between two groups, statistical analyses were performed by two-tailed unpaired Student's *t*-test. Comparison of multiple groups was made by one-way ANOVA, and statistical significance among multiple groups was determined by Tukey's post-hoc test (for pair-wise comparisons of means). All results are presented as mean ± SEM from at least three independent experiments.

3. Results

3.1. PDMS microgrooved substrates modulate MSC morphology

Cell morphology has been shown to serve as a key factor to guide MSC differentiation towards myogenic cell lineages, including SMCs [22]. To delineate the molecular mechanism by which elongated stem cell shape promotes SMC differentiation, we fabricated the culture substrates with parallel microgrooves with various widths (50, 25, and 10 μm)

and a depth of 10 μm using the soft lithography technique to modulate MSC morphology (Fig. 1A). MSCs were seeded onto the microgrooved or flat substrates for 24 h, followed by staining with FITC-phalloidin and DAPI to determine their cell and nuclear shape indices. To quantify the effect of microgrooves on cell morphology, we measured the shape indices as cell and nuclear areas, aspect ratios, and major and minor axis lengths of MSCs on those PDMS substrates. In comparison with the culture on a flat substrate, the cell bodies and nuclei of MSCs cultured on the microgrooves showed smaller areas and higher aspect ratio (i.e, more elongated) and became aligned along the microgrooves. Furthermore, the decreases in spreading areas and the increases in aspect ratios for both cell and nucleus became more pronounced as the width of microgrooves was reduced (Fig. 1B–D). The increases in the cell and nuclear aspect ratios were achieved mainly by the significant reductions in minor axis lengths (see major and minor axis statistics in Fig. SI1). Assessment of the effect of elongated cell shape on cytoskeletal tensions by immunostaining of myosin light chain 2 (MLC2) phosphorylation showed that the elongated cells on microgrooves had significantly higher MLC2 phosphorylation level with stress fibers alignment in comparison to the polygonal cells on the flat substrates (Fig. 1E). These results indicate that the microgrooves constrained MSC spreading, increased cytoskeletal tension, and promoted MSC elongation in a directional and width-dependent manner.

3.2. MSC elongation synergizes with TGF-β1 to promote MSC-to-SMC differentiation

Transforming growth factor-β1 (TGF-β1) is an important cytokine that promotes MSC differentiation into the myogenic lineage [22]. We tested the synergistic effect of cell morphology and TGF-β1 on MSC-to SMC differentiation by comparing the MSCs cultured on microgrooved and flat substrates under TGF-β1 treatment. As previously reported, TGF-β1 treatment induced MSC-to-SMC differentiation on the flat substrates after 3 days (Fig. 2A and SI2A), as indicated by the increases in the protein expressions of SMC markers: myosin heavy chain 11 (MYH11), α-smooth muscle actin (α-SMA), and smooth muscle protein-22 (SM-22). With the decreases in microgroove width, there were enhanced increases in the expressions of α-SMA and SM-22 in the presence of TGF-β1, and such increases were statistically significant in cells cultured on 10 μm microgrooved substrates (Fig. 2B). These findings were confirmed by western blot and qRT-PCR analyses (Figs. SI2A–B). Immunostaining of α-SMA expression in the differentiated cells showed that, in comparison to flat substrates, the 10 μm microgrooved substrates not only induced a significant increase of α-SMA protein level, but also the alignment of α-SMA bundles with the direction of the microgrooves (Fig. 2C). Altogether, our findings revealed a synergistic effect of 10 μm microgrooved substrates and TGF-β1 treatment in promoting MSC-to-SMC differentiation. In addition, the MSCs on 10 μm microgrooves showed the cell aspect ratio of 13:1 (Fig. 1C), which is comparable to the 9:1 to 15:1 aspect ratios observed for SMCs in vivo [23]. Hence, we focused on the studies of MSC-to-SMC differentiation using microgrooves with 10 μm width in the following experiments.

3.3. MSC elongation increased SMC marker expressions via the upregulation of miR-145

To explore the regulatory mechanism underlying the cell elongation-induced MSC-to-SMC differentiation, we analyzed miRNA expressions in MSCs cultured on the microgrooved or flat substrates in the presence of TGF-β1. Following a systematic literature review, we

selected 14 miRNAs previously implicated in the regulations of SMC phenotypic control and other myogenic processes and found that cell elongation caused significant increases of miR-133 and −145 and significant decreases of miR-1, −21, −27a and −27b, while miR-155, −206 and −208 showed increased trends but not statistically significant, and miR-486 and −499 were not detectable (Fig. 3A). We further determined the roles of these differentially expressed miRNAs in MSC-to-SMC differentiation. For MSCs on flat substrates, the overexpression of miR145, but not other up-regulated miRNAs, significantly induced the expression of α-SMA and SM-22 (Fig. 3B, left panel), while the knockdowns of miR-1, −21, −27a or −27b did not have any effect (Fig. 3B, right panel). These results suggest the importance of miR-145 in the induction of MSC-to-SMC differentiation by microgrooves. Further gain- and loss-of-function experiments were then performed by the transfection of pre-miR-145 precursor (PM145) or anti-miR-145 inhibitor (AM145), as well as their respective controls (PMC and AMC), into MSCs cultured on the microgrooved or flat substrates. The overexpression of miR-145 with PM145, mimicking the effect of the elongated cell shape on miR145, resulted in increases of α-SMA and SM-22 expressions even on the flat substrates, while inhibition of miR-145 with AM145 abolished the up-regulation of SMC markers in cells differentiated on the microgrooved substrates (Fig. 3C). To further delineate the mechanism by which the cell elongation-induced miR-145 promotes MSC-to-SMC differentiation, we examined the levels of miR-145 target genes involved in SMC biology, i.e., *Myo-CD, SSH2, MRTF, CAM2D, KLF4* and *KLF5*, in the miR-145-overexpressing MSCs on flat substrates. Our results showed that *SSH2, CAM2D* and *KLF4* were significantly downregulated by miR-145 overexpression (Fig. SI3). Among these target genes, KLF4 has been reported to play a significant role in modulating both stem cell pluripotency and SMC phenotypic switch [24,25]. Further experiments demonstrated that KLF4 was down-regulated in the MSCs on microgrooves in comparison to those on flat substrates, and that such reduction of KLF4 expression was abolished by AM145 (Fig. 3D). These findings indicate that miR-145 and KLF4 are important for the cell elongation-directed MSC-to-SMC differentiation.

3.4. Rho/ROCK pathway regulates cell shape elongation and directs MSC-to-SMC differentiation through miR-145/KLF4 axis

As shown in Fig. 1, culturing MSCs on microgrooves caused MLC2 phosphorylation and actin remodeling. Since MLC2 modulation of cytoskeletal organization is controlled by Rho/ROCK pathway [6], we examined the role of Rho/ROCK in MSC-to-SMC differentiation on the microgrooves by treating cells with C3 exoenzyme (a Rho inhibitor) or Y-27632 (a ROCK inhibitor) for 24 h, followed by staining of actin fibers and nuclei. In comparison to the control cells on microgrooves, C3 treatment caused a slight reduction in cell area with the cells remained confined within the microgrooved channels; Y-27632 treatment caused increases in cell and nuclear areas with the cells spread over the microgrooves and extended long and thin membrane protrusions from both ends of the cell (Fig. 4A–B). While the C3- and Y-27632-treated cells exhibited different trends of changes in cell and nuclear areas, both treatments significantly reduced cell and nuclear aspect ratios in comparison to the control cells on microgrooves (Fig. 4B and SI4). Both C3 and Y-27632 treatments impaired the cell elongation-induced MSC-to-SMC differentiation, as evidenced by the abolishment of the inductions of SMC markers and miR-145 and reduction of KLF4 in cells

cultured on the microgrooves (Fig. 4C–E). Importantly, we found that such C3 and Y-27632 inhibitory effects on SMC differentiation were reversed by the overexpression of miR-145 (Fig. 4F). These results demonstrate that the elongated cell shape-induced MSC-to-SMC differentiation through the Rho-ROCK/miR-145/KLF4 pathway and support the notion that the aspect ratios, but not areas, of cell and nucleus, are the key biomechanical factors regulating this process.

3.5. Induction of miR-145 promotes the contractility of SMCs differentiated on the microgrooved substrates

Contractility is an important indicator of the functional phenotype of SMCs [26]. To investigate whether microgrooved substrates provide a critical biophysical cue for the derivation of SMCs with high contractility, TFM was performed to measure the contractile forces exerted by the cells on substrates. MSCs were maintained in the basal medium or differentiated on the microgrooved or flat substrates for 3 days with TGF-β1 treatment, and then sub-cultured onto polyacrylamide gels for TFM analysis. The contractile forces exerted by the differentiated cells sub-cultured from microgrooves are significantly higher than those from the flat substrates or the MSCs in the basal medium (Fig. SI5), suggesting that the elongated cell shape enhances the differentiation of functional SMCs. The inhibition of miR-145 reduced the microgrooveinduced contractile forces, while overexpression of miR-145 augmented the contractile forces in the cells from flat substrates. These results showed that upregulation of miR-145 is necessary for the induction of contractile phenotype in the differentiated SMCs (Fig. 5A–B). Cell area did not undergo significant differences between the cells were sub-cultured from microgrooved or flat substrates. However, the cells sub-cultured from microgrooves retained more elongated cell shapes in comparison to those from flat substrates, and this retention of cell elongation was abolished by miR-145 knockdown (Fig. 5C). Altogether, our results demonstrate that the elongated cell shape promotes MSC differentiation toward contractile SMCs, and that this differentiation process is mediated by miR-145.

4. Discussion

Previous studies have shown that modulations of biophysical cues (such as cell morphology and cytoskeletal tension) and the stimulation of TGF-β1 can promote myogenic differentiation of MSCs [6,7,27]. While the role of TGF-β1 in SMC plasticity is better defined, the mechanism underlying the MSC-to-SMC differentiation induced by biophysical cues is still unknown [22,28]. In the current study, we employed the microgrooved substrates to impose an elongated MSC shape and induce an increased cytoskeletal tension, which are both critical for SMC differentiation. Most importantly, we demonstrate a novel mechanism by which the elongated cell and nuclear shapes direct MSC-toSMC differentiation through a Rho-ROCK/miR-145/KLF4 signaling pathway (Fig. 6).

Our approach to enhance MSC-to-SMC differentiation is to provide the biophysical microenvironments similar to where naïve SMCs reside [29]. The microgrooved substrates have been widely used in studies on cell differentiation in human blood vessels and myocardial tissues [10,28,30–35] (SI Table 2). However, the mechanisms for SMC

differentiation induced by MSC elongation are still not clearly understood. Our study employed substrates with different groove widths constituted an excellent platform to obtain elongated MSCs with the desired aspect ratios similar to contractile SMCs. Our results showed that MSCs aligned with the direction of microgrooves, and that the increase in cell aspect ratio and decrease in cell area were more pronounced in cells on the narrower microgrooved substrates (Fig. 1). In addition, 3-D imaging analysis showed a significant reduction in cell volume of MSCs on the microgrooved substrates (Fig. SI6). It has been reported that the conformational change of a cell can lead to the regulation of nuclear morphology and orientation through cytoskeletal reorganization [36]. Indeed, we noticed that the nuclei were deformed and oriented to the direction of microgrooves in a similar manner as the actin fiber and phospho-MLC2 stainings, suggesting that this deformation is caused by the increase in cytoskeletal tension (Fig. 1). It has been reported that nuclear deformation triggers gene expression not only at transcription and translation levels, but also through epigenetic modifications. For example, Li et al. showed that the elongated nuclear shape of MSC induces a high level of histone acetylation, thus regulating cell functions [28]. Here, we have shown that the increased cell aspect ratio resulted in nuclear elongation and served as a critical factor to promote MSC-to-SMC differentiation (Figs.1, 2 and 4). However, whether such a change in nuclear shape induces specific epigenetic modifications or chromatin remodeling to modulate MSC-to-SMC differentiation requires further investigation.

MiRNAs have been shown to serve as critical mechano-transducers in modulating stem cell fate [17–19,37]. In the current study, we hypothesized that biophysical cues affect miRNA expression to mediate MSC-to-SMC differentiation. We have demonstrated that elongation of MSCs induced the differential expressions of myogenic miRNAs, and that among those miRNAs, the up-regulation of miR-145 had the most profound effect on MSC-to-SMC differentiation. Although miR-143 is usually thought to be co-transcribed with miR-145, our data demonstrated that the miR-143 level was reduced in the elongated MSCs, suggesting the biogenesis of the miR-143/−145 cluster might involve a more complicated mechanism than previously appreciated. MiR-145 has been reported to serve as a multivalent regulator in both stem cells and SMCs. In embryonic stem cells, miR-145 represses self-renewal to decrease stemness, and in MSCs, miR-145 is a negative regulator of osteogenic and chondrogenic differentiation [38–40]. In SMCs, miR145 is one of the most abundant miRNAs, and induction of miR-145 under TGF-β1 treatment promotes contractile phenotype of SMCs [41]. Moreover, miR-145 has been recognized as a mechano-sensitive miRNA for shear stress- and stretch-modulated SMC phenotypes [18,42]. Consistent with these findings, our data revealed for the first time that increased aspect ratios in the cell bodies and nuclei up-regulated miR145 to promote MSC-to-SMC differentiation, and that inhibition of miR145 abolished this effect on differentiation (Fig. 3C). Among the functional targets of miR-145, KLF4 has been identified as a negative regulator of contractile phenotype by inhibiting α-SMA and SM-22 transcriptions [43]. Our gain- and loss-of-function experiments also demonstrated an inverse relation between KLF4 and miR-145 levels, suggesting the KLF4 inhibition by miR-145 mediates the MSC-to-SMC differentiation induced by cell elongation (Fig. 3D).

Rho/ROCK has been demonstrated to play an important role in stem cell differentiation, and it has been suggested that cytoskeletal remodeling and intracellular tension modulation are essential for lineage commitment [6,44,45]. Specifically, it has been reported that the activation of Rho/ROCK pathway increases cytoskeletal tensions to promote the MSC differentiation to myogenic and/or osteogenic lineages, while inhibition of Rho/ROCK favors adipogenic lineage [6,7,46]. In line with these findings, we found that the elongated cells on the microgrooved substrates exhibited higher levels of MLC2 phosphorylation and SMC markers, compared to the cells on flat substrates (Fig. 1E). Inhibition of Rho slightly decreased cell area on 10 μm microgrooved substrates compared with the control group; in contrast, inhibition of ROCK led to a significant larger cell area beyond the microgroove constraint (Fig. 4A–B and SI4). Thus, Rho and ROCK inhibitions caused distinct effects on cell area modulation in MSCs. However, both Rho and ROCK inhibitions reduced the cell and nuclear elongations and abolished the up-regulations of miR-145 and SMC markers, suggesting that the elongated shapes of cell and nucleus, but not spreading area, are crucial for MSC-to-SMC differentiation. Moreover, overexpression of miR-145 effectively restored the expression of SMC markers even in the presence of Rho and ROCK inhibitors, demonstrating that miR-145 is a downstream mechano-transducer of Rho/ROCK signaling. Taken together, our findings establish that MSC elongation induces SMC differentiation through the Rho-ROCK/miR-145/KLF4 regulatory pathway.

One of the most important functional characteristics of SMCs is that they exert large contractile forces in the maintenance of vascular tone and tissue remodeling. Using TFM to quantify the contractility induced by SMC differentiation, we found that the elongated cells cultured on microgrooves exerted significantly higher traction forces than those on flat substrates (Fig. SI5). Our findings suggest that the morphological modulation enhances functional SMC differentiation. Consistent with this notion, we found that overexpression of miR-145 mimicked the effect of cell elongation to increase cellular force exertion, whereas inhibition of miR-145 had an opposite effect. These results indicate that miR-145 is not only a mechano-sensitive molecule, but also essential for induction of contractile SMCs (Fig. 5A–B). Moreover, when sub-cultured to flat surfaces of polyacrylamide gels after 3 days culturing on the microgrooves, the cells still preserved the elongated morphology. (Fig. 5C), suggesting that they maintain the contractile feature of SMCs and thus have a great potential to be used in tissue engineering applications.

MSCs are an important source to generate SMCs for cell-based therapeutics, and the understanding of biophysical and biochemical cues to control SMC differentiation can significantly advance our ability to obtain sufficient amounts of functional SMCs. This study demonstrates the induction of an elongated MSC shape using an engineered microgroove substrate, in conjunction with TGF-β1 treatment, led to an improvement of SMC differentiation with better contractility through the Rho-ROCK/miR-145/KLF4-mediated signaling. These findings provide new insights to the mechanisms underlying the biophysical and biochemical regulations of MSC differentiation into SMC lineages and contribute to the development of bioengineering strategies for the treatment of vascular diseases.

Supplementary Material

Refer to Web version on PubMed Central for supplementary material.

Acknowledgements

This work was supported by funding from National Institutes of Health grants HL106579, HL108735, and HL121365 to S.C. and HL135416 to K.-C.W.; the American Heart Association Postdoctoral Fellowship POST33460467 and Career Development Award CDA34110462 to Y.-T.Y.; and UCSD Frontiers of Innovation Scholar Programs to S.C. and K.-C.W. This work was performed in part at the San Diego Nanotechnology Infrastructure (SDNI) of UCSD, a member of the National Nanotechnology Coordinated Infrastructure supported by the National Science Foundation (Grant ECCS-1542148).

References

[1]. Alexander MR, Owens GK, Epigenetic control of smooth muscle cell differentiation and phenotypic switching in vascular development and disease, Annu. Rev. Physiol. 74 (2012) 13–40. [PubMed: 22017177]

[2]. Wan M, Li C, Zhen G, Jiao K, He W, Jia X, Wang W, Shi C, Xing Q, Chen YF, Jan De Beur S, Yu B, Cao X, Injury-activated transforming growth factor beta controls mobilization of mesenchymal stem cells for tissue remodeling, Stem Cell. 30 (11) (2012) 2498–2511.

[3]. Li C, Zhen G, Chai Y, Xie L, Crane JL, Farber E, Farber CR, Luo X, Gao P, Cao X, Wan M, RhoA determines lineage fate of mesenchymal stem cells by modulating CTGF-VEGF complex in extracellular matrix, Nat. Commun. 7 (2016) 11455. [PubMed: 27126736]

[4]. Gu W, Hong X, Le Bras A, Nowak WN, Bhaloo S.Issa, Deng J, Xie Y, Hu Y, Ruan XZ, Xu Q, Smooth muscle cells differentiated from mesenchymal stem cells are regulated by microRNAs and suitable for vascular tissue grafts, J. Biol. Chem. 293 (21) (2018) 8089–8102. [PubMed: 29643181]

[5]. Engler AJ, Sen S, Sweeney HL, Discher DE, Matrix elasticity directs stem cell lineage specification, Cell 126 (4) (2006) 677–689. [PubMed: 16923388]

[6]. McBeath R, Pirone DM, Nelson CM, Bhadriraju K, Chen CS, Cell shape, cytoskeletal tension, and RhoA regulate stem cell lineage commitment, Dev. Cell 6 (4) (2004) 483–495. [PubMed: 15068789]

[7]. Kilian KA, Bugarija B, Lahn BT, Mrksich M, Geometric cues for directing the differentiation of mesenchymal stem cells, Proc. Natl. Acad. Sci. U. S. A. 107 (11) (2010) 4872–4877. [PubMed: 20194780]

[8]. Tay CY, Wu YL, Cai P, Tan NS, Venkatraman SS, Chen X, Tan LP, Bio-inspired micropatterned hydrogel to direct and deconstruct hierarchical processing of geometry-force signals by human mesenchymal stem cells during smooth muscle cell differentiation, NPG Asia Mater. 7 (2015) e199.

[9]. Jang JY, Lee SW, Park SH, Shin JW, Mun C, Kim SH, Kim DH, Shin JW, Combined effects of surface morphology and mechanical straining magnitudes on the differentiation of mesenchymal stem cells without using biochemical reagents, J. Biomed. Biotechnol. 2011 (2011) 860652.

[10]. Chang S, Song S, Lee J, Yoon J, Park J, Choi S, Park JK, Choi K, Choi C, Phenotypic modulation of primary vascular smooth muscle cells by short-term culture on micropatterned substrate, PLoS One 9 (2) (2014) e88089.

[11]. Gangaraju VK, Lin H, MicroRNAs: key regulators of stem cells, Nat. Rev. Mol. Cell Biol. 10 (2) (2009) 116–125. [PubMed: 19165214]

[12]. Rao PK, Kumar RM, Farkhondeh M, Baskerville S, Lodish HF, Myogenic factors that regulate expression of muscle-specific microRNAs, Proc. Natl. Acad. Sci. U. S. A. 103 (23) (2006) 8721–8726. [PubMed: 16731620]

[13]. Welten SM, Goossens EA, Quax PH, Nossent AY, The multifactorial nature of microRNAs in vascular remodelling, Cardiovasc. Res. 110 (1) (2016) 6–22. [PubMed: 26912672]

[14]. Joshi SR, Comer BS, McLendon JM, Gerthoffer WT, MicroRNA regulation of smooth muscle phenotype, Mol. Cell. Pharmacol. 4 (1) (2012) 1–16. [PubMed: 25309675]

[15]. Cordes KR, Sheehy NT, White MP, Berry EC, Morton SU, Muth AN, Lee TH, Miano JM, Ivey KN, Srivastava D, miR-145 and miR-143 regulate smooth muscle cell fate and plasticity, Nature 460 (7256) (2009) 705–710. [PubMed: 19578358]

[16]. Pajoohesh M, Naderi-Manesh H, Soleimani M, MicroRNA-145-based differentiation of human mesenchymal stem cells to smooth muscle cells, Biotechnol. Lett. 38 (11) (2016) 1975–1981. [PubMed: 27439694]

[17]. Neth P, Nazari-Jahantigh M, Schober A, Weber C, MicroRNAs in flow-dependent vascular remodelling, Cardiovasc. Res. 99 (2) (2013) 294–303. [PubMed: 23612583]

[18]. Hu B, Song JT, Qu HY, Bi CL, Huang XZ, Liu XX, Zhang M, Mechanical stretch suppresses microRNA-145 expression by activating extracellular signalregulated kinase 1/2 and upregulating angiotensin-converting enzyme to alter vascular smooth muscle cell phenotype, PLoS One 9 (5) (2014) e96338.

[19]. Wang KC, Garmire LX, Young A, Nguyen P, Trinh A, Subramaniam S, Wang N, Shyy JY, Li YS, Chien S, Role of microRNA-23b in flow-regulation of Rb phosphorylation and endothelial cell growth, Proc. Natl. Acad. Sci. U. S. A. 107 (7) (2010) 3234–3239. [PubMed: 20133741]

[20]. Del Alamo JC, Meili R, Alonso-Latorre B, Rodriguez-Rodriguez J, Aliseda A, Firtel RA, Lasheras JC, Spatio-temporal analysis of eukaryotic cell motility by improved force cytometry, Proc. Natl. Acad. Sci. U. S. A. 104 (33) (2007) 13343–13348. [PubMed: 17684097]

[21]. del Alamo JC, Meili R, Alvarez-Gonzalez B, Alonso-Latorre B, Bastounis E, Firtel R, Lasheras JC, Three-dimensional quantification of cellular traction forces and mechanosensing of thin substrata by fourier traction force microscopy, PLoS One 8 (9) (2013) e69850.

[22]. Kurpinski K, Lam H, Chu J, Wang A, Kim A, Tsay E, Agrawal S, Schaffer DV, Li S, Transforming growth factor-beta and notch signaling mediate stem cell differentiation into smooth muscle cells, Stem Cell. 28 (4) (2010) 734–742.

[23]. Rhodin JAG, Architecture of the vessel wall, Compressive Physiology, (1980).

[24]. Zhang P, Andrianakos R, Yang Y, Liu C, Lu W, Kruppel-like factor 4 (Klf4) prevents embryonic stem (ES) cell differentiation by regulating Nanog gene expression, J. Biol. Chem. 285 (12) (2010) 9180–9189. [PubMed: 20071344]

[25]. Shankman LS, Gomez D, Cherepanova OA, Salmon M, Alencar GF, Haskins RM, Swiatlowska P, Newman AA, Greene ES, Straub AC, Isakson B, Randolph GJ, Owens GK, KLF4-dependent phenotypic modulation of smooth muscle cells has a key role in atherosclerotic plaque pathogenesis, Nat. Med. 21 (6) (2015) 628–637. [PubMed: 25985364]

[26]. Beamish JA, He P, Kottke-Marchant K, Marchant RE, Molecular regulation of contractile smooth muscle cell phenotype: implications for vascular tissue engineering, Tissue Eng. B Rev. 16 (5) (2010) 467–491.

[27]. Yang Y, Relan NK, Przywara DA, Schuger L, Embryonic mesenchymal cells share the potential for smooth muscle differentiation: myogenesis is controlled by the cell's shape, Development 126 (13) (1999) 3027–3033. [PubMed: 10357945]

[28]. Li Y, Chu JS, Kurpinski K, Li X, Bautista DM, Yang L, Sung KL, Li S, Biophysical regulation of histone acetylation in mesenchymal stem cells, Biophys. J. 100 (8) (2011) 1902–1909. [PubMed: 21504726]

[29]. Guilak F, Cohen DM, Estes BT, Gimble JM, Liedtke W, Chen CS, Control of stem cell fate by physical interactions with the extracellular matrix, Cell Stem Cell 5 (1) (2009) 17–26. [PubMed: 19570510]

[30]. Heidi Au HT, Cui B, Chu ZE, Veres T, Radisic M, Cell culture chips for simultaneous application of topographical and electrical cues enhance phenotype of cardiomyocytes, Lab Chip 9 (4) (2009) 564–575. [PubMed: 19190792]

[31]. Saito AC, Matsui TS, Ohishi T, Sato M, Deguchi S, Contact guidance of smooth muscle cells is associated with tension-mediated adhesion maturation, Exp. Cell Res. 327 (1) (2014) 1–11. [PubMed: 24825188]

[32]. Kurpinski K, Chu J, Hashi C, Li S, Anisotropic mechanosensing by mesenchymal stem cells, Proc. Natl. Acad. Sci. U. S. A. 103 (44) (2006) 16095–16100. [PubMed: 17060641]

[33]. Sia J, Yu P, Srivastava D, Li S, Effect of biophysical cues on reprogramming to cardiomyocytes, Biomaterials 103 (2016) 1–11. [PubMed: 27376554]

[34]. Fu FF, Shang LR, Chen ZY, Yu YR, Zhao YJ, Bioinspired living structural color hydrogels, Sci. Robot. 3 (16) (2018).

[35]. Chen S, Kawazoe N, Chen G, Biomimetic assembly of vascular endothelial cells and muscle cells in microgrooved collagen porous scaffolds, Tissue Eng. C Methods 23 (6) (2017) 367–376.

[36]. Versaevel M, Grevesse T, Gabriele S, Spatial coordination between cell and nuclear shape within micropatterned endothelial cells, Nat. Commun. 3 (2012) 671. [PubMed: 22334074]

[37]. Frith JE, Kusuma GD, Carthew J, Li F, Cloonan N, Gomez GA, CooperWhite JJ, Mechanically-sensitive miRNAs bias human mesenchymal stem cell fate via mTOR signalling, Nat. Commun. 9 (1) (2018) 257. [PubMed: 29343687]

[38]. Yu Z, Li Y, Fan H, Liu Z, Pestell RG, miRNAs regulate stem cell self-renewal and differentiation, Front. Genet. 3 (2012) 191. [PubMed: 23056008]

[39]. Choi E, Choi E, Hwang KC, MicroRNAs as novel regulators of stem cell fate, World J. Stem Cell. 5 (4) (2013) 172–187.

[40]. Yang B, Guo H, Zhang Y, Chen L, Ying D, Dong S, MicroRNA-145 regulates chondrogenic differentiation of mesenchymal stem cells by targeting Sox9, PLoS One 6 (7) (2011) e21679.

[41]. Riches K, Alshanwani AR, Warburton P, O'Regan DJ, Ball SG, Wood IC, Turner NA, Porter KE, Elevated expression levels of miR-143/5 in saphenous vein smooth muscle cells from patients with Type 2 diabetes drive persistent changes in phenotype and function, J. Mol. Cell. Cardiol. 74 (2014) 240–250. [PubMed: 24927876]

[42]. Hergenreider E, Heydt S, Treguer K, Boettger T, Horrevoets AJ, Zeiher AM, Scheffer MP, Frangakis AS, Yin X, Mayr M, Braun T, Urbich C, Boon RA, Dimmeler S, Atheroprotective communication between endothelial cells and smooth muscle cells through miRNAs, Nat. Cell Biol. 14 (3) (2012) 249–256. [PubMed: 22327366]

[43]. Liu Y, Sinha S, McDonald OG, Shang Y, Hoofnagle MH, Owens GK, Kruppellike factor 4 abrogates myocardin-induced activation of smooth muscle gene expression, J. Biol. Chem. 280 (10) (2005) 9719–9727. [PubMed: 15623517]

[44]. Keung AJ, de Juan-Pardo EM, Schaffer DV, Kumar S, Rho GTPases mediate the mechanosensitive lineage commitment of neural stem cells, Stem Cell. 29 (11) (2011) 1886–1897.

[45]. Maharam E, Yaport M, Villanueva NL, Akinyibi T, Laudier D, He Z, Leong DJ, Sun HB, Rho/Rock signal transduction pathway is required for MSC tenogenic differentiation, Bone Res. 3 (2015) 15015.

[46]. Eyckmans J, Lin GL, Chen CS, Adhesive and mechanical regulation of mesenchymal stem cell differentiation in human bone marrow and periosteum-derived progenitor cells, Biol. Open 1 (11) (2012) 1058–1068. [PubMed: 23213385]

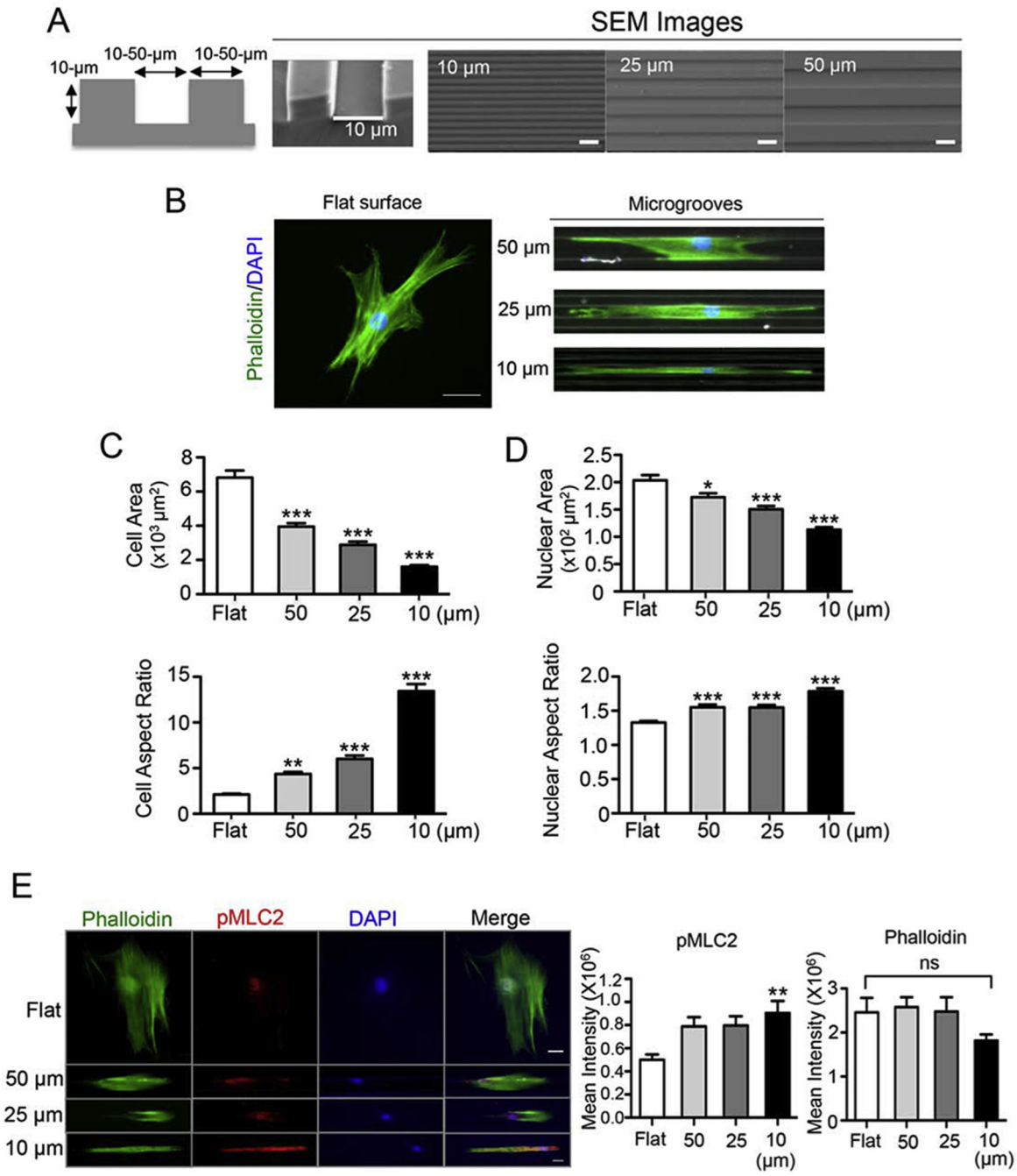

Fig. 1. Microgrooved substrates impose elongated cell shape in MSCs.

(A) SEM images of PDMS substrates with parallel microgrooves (10, 25, and 50 μm in width, and 10 μm in height). PDMS microgrooved substrates were fabricated and coated with FN as described in the Materials and Methods. Scale = 50 μm. (B) MSCs were cultured on PDMS flat or microgrooved substrates for 24 h and stained with FITC-phalloidin (green) for cell morphology and DAPI (blue) for nuclei. Scale = 20 μm. (C) Quantification of total cell area and aspect ratio were shown in four groups as flat and microgrooved substrates with 50, 25 and 10 μm widths. (D) Quantification of nuclear area and aspect ratio in the

four groups were shown. Data are presented as mean ± SEM,with 40–60 cells in each group; * vs. the corresponding flat substrates, *P < 0.05, **P < 0.005, ***P < 0.0001. (E) Immunofluorescence stainings of MLC2 phosphorylation (pMLC2), FITC-phalloidin, and DAPI in MSCs cultured on flat or microgrooved substrates with 50, 25 and 10 μm widths. Scale bar = 20 μm. The graphic data are mean ± SEM of pMLC2 and FITC-phalloidin from at least 26 cells randomly selected. * vs. flat substrates, **P < 0.005.

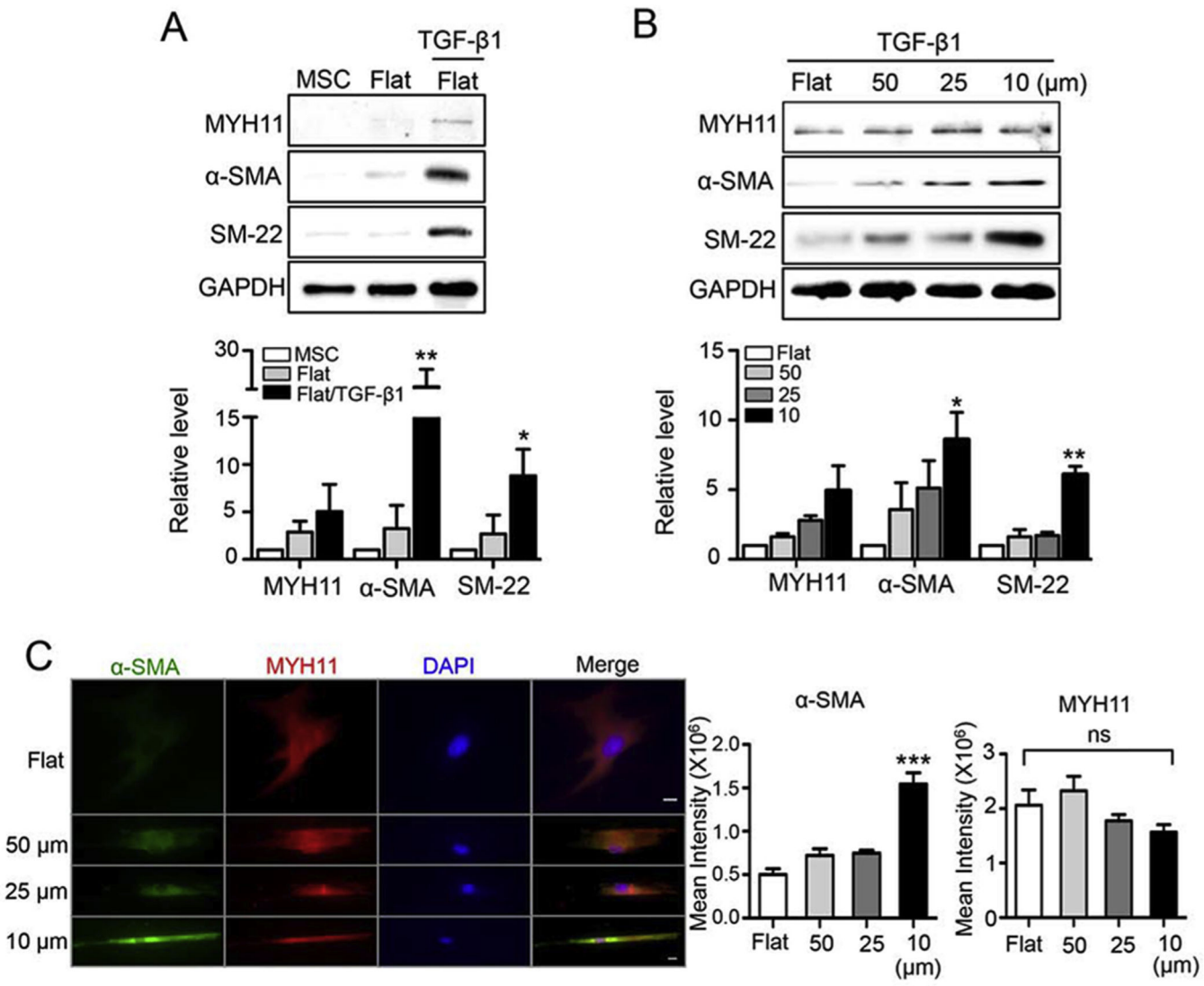

Fig. 2. Elongated cell shape increases SMC marker expressions and cytoskeletal tensions.

(A) Western blot analyses of MYH11, α-SMA, SM-22 and GAPDH in MSCs cultured in basal MSCGM or DMEM medium without or with TGF-β1 for 3 days. The graphic data are mean ± SEM of band intensity normalized to MSC control, n = 3. *P < 0.05, **P < 0.005. (B) Western blot analyses of MYH11, α-SMA, SM-22 and GAPDH in MSCs cultured on flat or microgrooved substrates with 50, 25 and 10 μm widths in DMEM medium with TGF-β1 for 3 days. The graphic data are mean ± SEM of band intensity normalized to flat control, n = 3. *P < 0.05, **P < 0.005. (C) Immunofluorescence stainings of α-SMA, MYH11, and DAPI in MSCs cultured on flat or microgrooved substrates with 50, 25 and 10μm widths in DMEM medium with TGF-β1 for 3 days. Scale bar = 20 μm. The graphic data are mean ± SEM of the α-SMA and MYH11 intensity ratios from at least 15 cells randomly selected from three independent experiments. * vs. flat substrates, ***P < 0.0001.

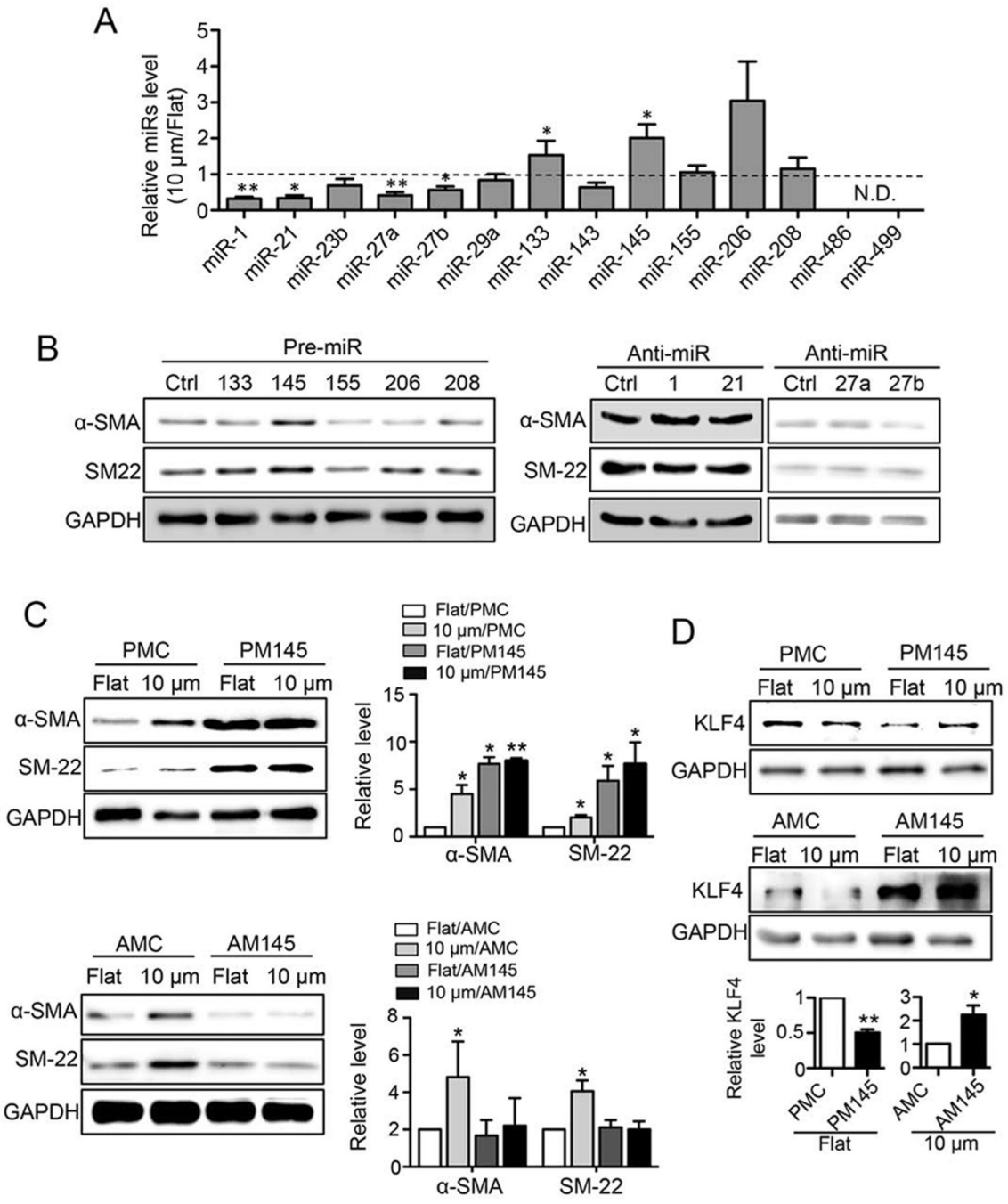

Fig. 3. Elongated cell shape induces SMC differentiation through the miR-145/KLF4 pathway.

(A) MicroRNA expression analyses in MSCs subjected to flat or 10 μm microgrooved substrates with TGF-β1 for 3 days. The microgroove-regulated miRNAs expressions were examined by qRT-PCR. The graphic data is mean ± SEM of value normalized to flat substrates, n = 3. *P < 0.05, **P < 0.005. (B) Western blot analyses of α-SMA, SM-22 and GAPDH in MSCs transfected with microgroove-regulated miRNAs or the corresponding controls on flat substrates with TGF-β1 for 3 days. (C) Western blot analyses of α-SMA, SM-22 and GAPDH in MSCs transfected with PM145, AM145 or the corresponding

controls and cultured on flat or 10 μm microgrooved substrates. The graphic data are mean ± SEM of band intensity normalized to flat control, n = 3. *P < 0.05, **P < 0.005. (D) Western blot analyses of KLF4 and GAPDH in MSCs transfected with PM145, AM145 or the corresponding controls and cultured on flat or 10 μm microgrooved substrates. The graphic data are mean ± SEM of band intensity normalized to control, n = 3. *P < 0.05, **P < 0.005.

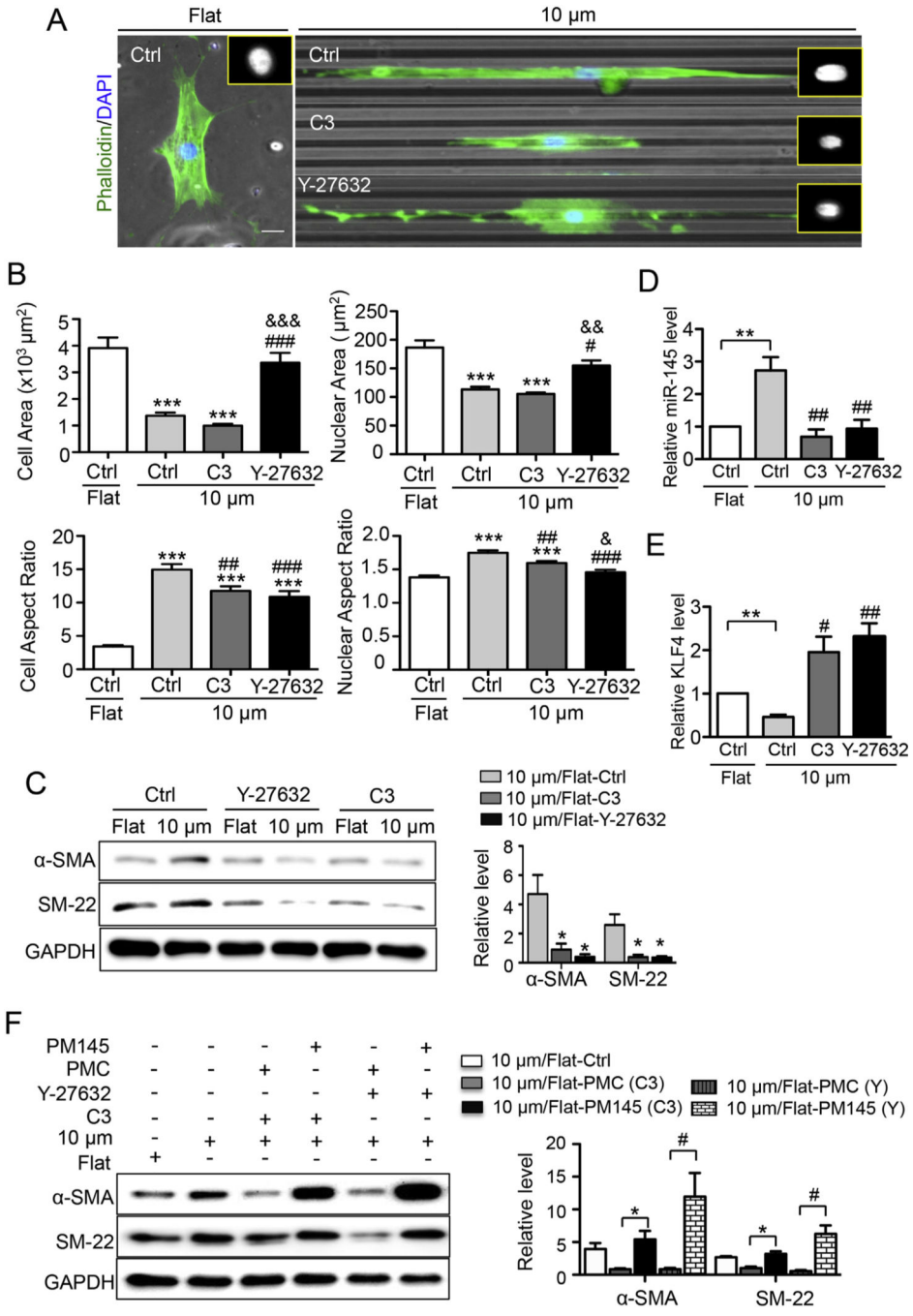

Fig. 4. Rho/ROCK signaling regulates miR-145/KLF4 to mediate the cell elongation-induced MSC-to-SMC differentiation.

(A) MSCs were cultured on flat or 10 μm microgrooved substrates and treated without or with C3 or Y-27632 for 24 h, followed by stainings with FITC-phalloidin for cell morphology and DAPI for nuclei. Scale = 20 μm. (B) Quantification of total cell area, cell body aspect ratio, nuclear area and nuclear aspect ratio in the four groups were shown. Data are presented as the mean ± SEM, with 35–55 cells in each group. * vs. flat control, ***$P < 0.0001$. # vs. 10 μm microgrooved control, #$P < 0.05$, ##$P < 0.005$, ###$P < 0.0001$. & vs. C3 treated group, &$P < 0.05$, &&$P < 0.005$, &&&$P < 0.0001$. (C) Western blot analyses

of α-SMA, SM-22 and GAPDH in MSCs treated with C3, Y-27632 or the vehicle control and cultured on flat or microgrooved substrates. The graphic data are mean ± SEM of band intensity normalized to flat control, n = 3. *P < 0.05. (D) MiR-145 expression in MSCs treated with C3, Y-27632, or the vehicle control and cultured on flat or microgrooved substrates. n = 3. * vs. flat control, **P < 0.005. # vs 10 μm microgrooved control, ##P < 0.005. (E) qRT-PCR analysis of KLF4 gene expression in MSCs treated with C3, Y27632, or the vehicle control and cultured on flat or microgrooved substrates. n = 3. * vs. flat control, **P < 0.005. # vs 10 μm microgrooved control, #P < 0.05, ##P < 0.005. (F) Western blot analyses of α-SMA, SM-22, and GAPDH in MSCs treated with C3 or Y27632 and transfected with PM145 or PMC control and cultured on flat or microgrooved substrates. The graphic data are mean ± SEM of band intensity normalized to flat control, n = 3. * vs. PMC in C3 treated group, *P < 0.05; # vs. PMC in Y-27632 treated group, #P < 0.05.

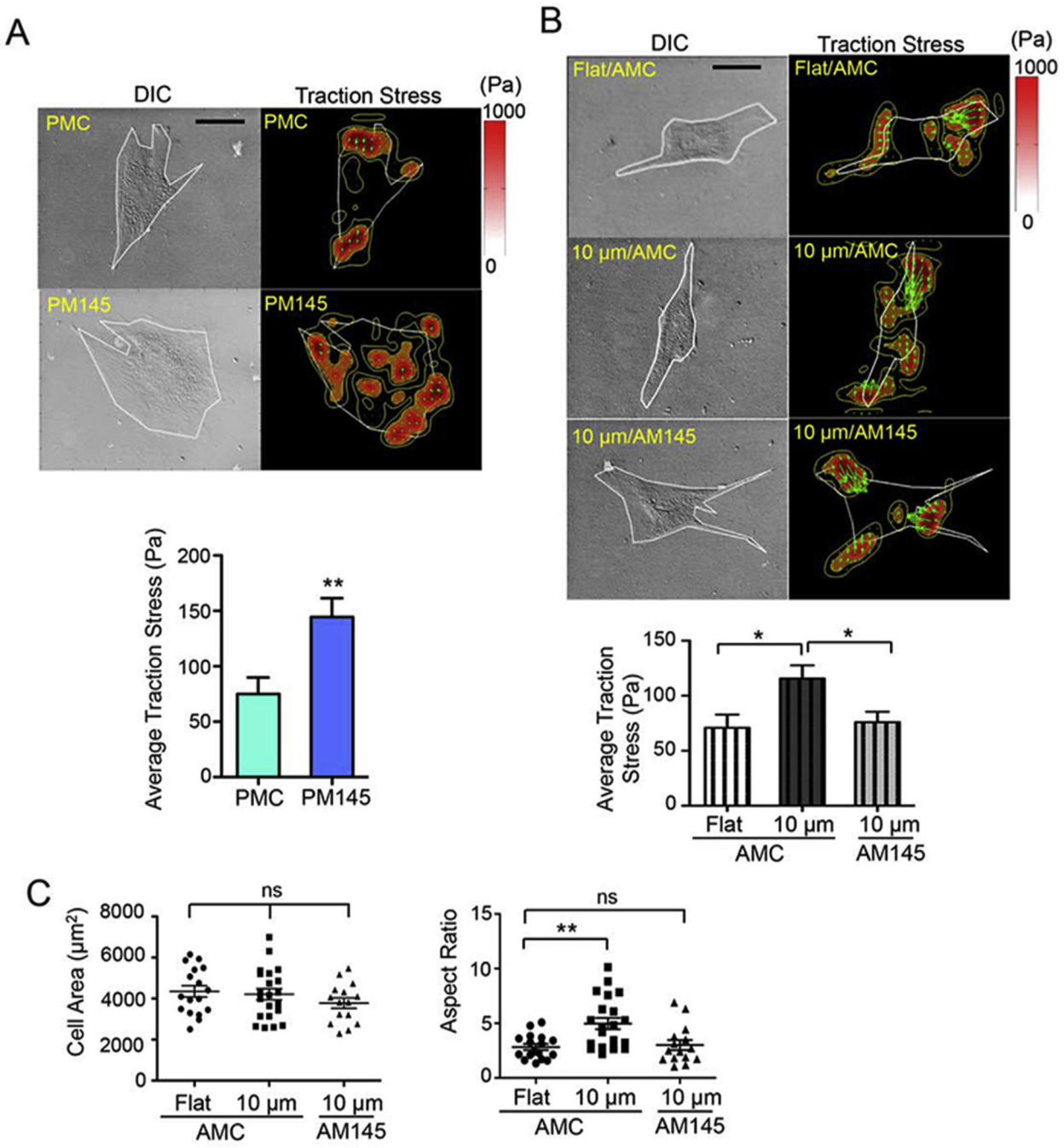

Fig. 5. MiR-145 is essential in the induction of contractile SMCs.

(A–B) MSCs were transfected with PM145, AM145, or the corresponding controls, followed by differentiation on flat or 10 μm microgrooved substrates for 3 days. The cells were then sub-cultured onto the polyacrylamide gels for the measurement of traction stresses. Upper panel: representative images of cell traction stresses exerted on the polyacrylamide gels. The stress magnitude is presented by the color bar (pascal), and green arrows represent stress vector directions. Scale = 100 μm. Lower panel: quantification of traction stresses. Data are presented as mean ± SEM of three independent experiments. 14–

20 cells from each group were analyzed. *P < 0.05, **P < 0.005. (C) Quantification of cell area and cell aspect ratio in cells which were transfected with AM145 or AMC, followed by differentiation on flat or 10 μm microgrooved substrates for 3 days and subcultured on the polyacrylamide gels. Data are presented as mean ± SEM of three independent experiments. 14–20 cells from each group were analyzed. **P < 0.005.

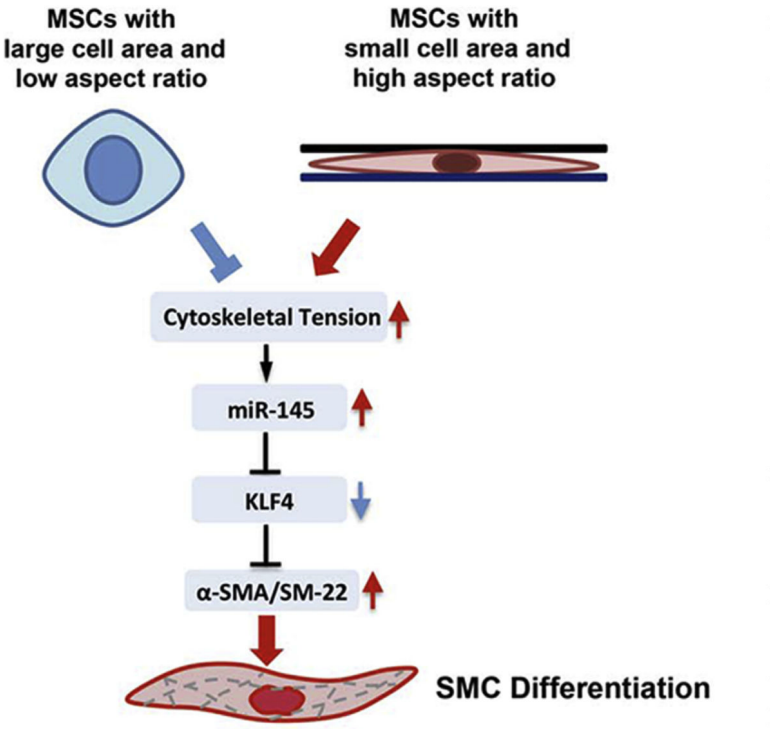

Fig. 6.

Schematic diagram of the signaling axis in mediating the elongated cell shape-induced MSC-to-SMC differentiation.